Improved Measurement of $B^+ \to \rho^+\rho^0$ and Determination of the Quark-Mixing Phase Angle α

B. Aubert,[1] Y. Karyotakis,[1] J. P. Lees,[1] V. Poireau,[1] E. Prencipe,[1] X. Prudent,[1] V. Tisserand,[1] J. Garra Tico,[2] E. Grauges,[2] L. Lopez,[3a,3b] A. Palano,[3a,3b] M. Pappagallo,[3a,3b] G. Eigen,[4] B. Stugu,[4] L. Sun,[4] M. Battaglia,[5] D. N. Brown,[5] L. T. Kerth,[5] Yu. G. Kolomensky,[5] G. Lynch,[5] I. L. Osipenkov,[5] K. Tackmann,[5] T. Tanabe,[5] C. M. Hawkes,[6] N. Soni,[6] A. T. Watson,[6] H. Koch,[7] T. Schroeder,[7] D. J. Asgeirsson,[8] B. G. Fulsom,[8] C. Hearty,[8] T. S. Mattison,[8] J. A. McKenna,[8] M. Barrett,[9] A. Khan,[9] A. Randle-Conde,[9] V. E. Blinov,[10] A. D. Bukin,[10] A. R. Buzykaev,[10] V. P. Druzhinin,[10] V. B. Golubev,[10] A. P. Onuchin,[10] S. I. Serednyakov,[10] Yu. I. Skovpen,[10] E. P. Solodov,[10] K. Yu. Todyshev,[10] M. Bondioli,[11] S. Curry,[11] I. Eschrich,[11] D. Kirkby,[11] A. J. Lankford,[11] P. Lund,[11] M. Mandelkern,[11] E. C. Martin,[11] D. P. Stoker,[11] S. Abachi,[12] C. Buchanan,[12] H. Atmacan,[13] J. W. Gary,[13] F. Liu,[13] O. Long,[13] G. M. Vitug,[13] Z. Yasin,[13] L. Zhang,[13] V. Sharma,[14] C. Campagnari,[15] T. M. Hong,[15] D. Kovalskyi,[15] M. A. Mazur,[15] J. D. Richman,[15] T. W. Beck,[16] A. M. Eisner,[16] C. A. Heusch,[16] J. Kroseberg,[16] W. S. Lockman,[16] A. J. Martinez,[16] T. Schalk,[16] B. A. Schumm,[16] A. Seiden,[16] L. O. Winstrom,[16] C. H. Cheng,[17] D. A. Doll,[17] B. Echenard,[17] F. Fang,[17] D. G. Hitlin,[17] I. Narsky,[17] T. Piatenko,[17] F. C. Porter,[17] R. Andreassen,[18] G. Mancinelli,[18] B. T. Meadows,[18] K. Mishra,[18] M. D. Sokoloff,[18] P. C. Bloom,[19] W. T. Ford,[19] A. Gaz,[19] J. F. Hirschauer,[19] M. Nagel,[19] U. Nauenberg,[19] J. G. Smith,[19] S. R. Wagner,[19] R. Ayad,[20,*] A. Soffer,[20,†] W. H. Toki,[20] R. J. Wilson,[20] E. Feltresi,[21] A. Hauke,[21] H. Jasper,[21] M. Karbach,[21] J. Merkel,[21] A. Petzold,[21] B. Spaan,[21] K. Wacker,[21] M. J. Kobel,[22] R. Nogowski,[22] K. R. Schubert,[22] R. Schwierz,[22] A. Volk,[22] D. Bernard,[23] G. R. Bonneaud,[23] E. Latour,[23] M. Verderi,[23] P. J. Clark,[24] S. Playfer,[24] J. E. Watson,[24] M. Andreotti,[25a,25b] D. Bettoni,[25a] C. Bozzi,[25a] R. Calabrese,[25a,25b] A. Cecchi,[25a,25b] G. Cibinetto,[25a,25b] P. Franchini,[25a,25b] E. Luppi,[25a,25b] M. Negrini,[25a,25b] A. Petrella,[25a,25b] L. Piemontese,[25a] V. Santoro,[25a,25b] R. Baldini-Ferroli,[26] A. Calcaterra,[26] R. de Sangro,[26] G. Finocchiaro,[26] S. Pacetti,[26] P. Patteri,[26] I. M. Peruzzi,[26,‡] M. Piccolo,[26] M. Rama,[26] A. Zallo,[26] R. Contri,[27a,27b] E. Guido,[27a,27b] M. Lo Vetere,[27a,27b] M. R. Monge,[27a,27b] S. Passaggio,[27a] C. Patrignani,[27a,27b] E. Robutti,[27a] S. Tosi,[27a,27b] K. S. Chaisanguanthum,[28] M. Morii,[28] A. Adametz,[29] J. Marks,[29] S. Schenk,[29] U. Uwer,[29] F. U. Bernlochner,[30] V. Klose,[30] H. M. Lacker,[30] D. J. Bard,[31] P. D. Dauncey,[31] M. Tibbetts,[31] P. K. Behera,[32] X. Chai,[32] M. J. Charles,[32] U. Mallik,[32] J. Cochran,[33] H. B. Crawley,[33] L. Dong,[33] W. T. Meyer,[33] S. Prell,[33] E. I. Rosenberg,[33] A. E. Rubin,[33] Y. Y. Gao,[34] A. V. Gritsan,[34] Z. J. Guo,[34] N. Arnaud,[35] J. Béquilleux,[35] A. D'Orazio,[35] M. Davier,[35] J. Firmino da Costa,[35] G. Grosdidier,[35] F. Le Diberder,[35] V. Lepeltier,[35] A. M. Lutz,[35] S. Pruvot,[35] P. Roudeau,[35] M. H. Schune,[35] J. Serrano,[35] V. Sordini,[35,§] A. Stocchi,[35] G. Wormser,[35] D. J. Lange,[36] D. M. Wright,[36] I. Bingham,[37] J. P. Burke,[37] C. A. Chavez,[37] J. R. Fry,[37] E. Gabathuler,[37] R. Gamet,[37] D. E. Hutchcroft,[37] D. J. Payne,[37] C. Touramanis,[37] A. J. Bevan,[38] C. K. Clarke,[38] F. Di Lodovico,[38] R. Sacco,[38] M. Sigamani,[38] G. Cowan,[39] S. Paramesvaran,[39] A. C. Wren,[39] D. N. Brown,[40] C. L. Davis,[40] A. G. Denig,[41] M. Fritsch,[41] W. Gradl,[41] A. Hafner,[41] K. E. Alwyn,[42] D. Bailey,[42] R. J. Barlow,[42] G. Jackson,[42] G. D. Lafferty,[42] T. J. West,[42] J. I. Yi,[42] J. Anderson,[43] C. Chen,[43] A. Jawahery,[43] D. A. Roberts,[43] G. Simi,[43] J. M. Tuggle,[43] C. Dallapiccola,[44] E. Salvati,[44] S. Saremi,[44] R. Cowan,[45] D. Dujmic,[45] P. H. Fisher,[45] S. W. Henderson,[45] G. Sciolla,[45] M. Spitznagel,[45] R. K. Yamamoto,[45] M. Zhao,[45] P. M. Patel,[46] S. H. Robertson,[46] M. Schram,[46] A. Lazzaro,[47a,47b] V. Lombardo,[47a] F. Palombo,[47a,47b] S. Stracka,[47a,47b] J. M. Bauer,[48] L. Cremaldi,[48] R. Godang,[48,‖] R. Kroeger,[48] D. J. Summers,[48] H. W. Zhao,[48] M. Simard,[49] P. Taras,[49] H. Nicholson,[50] G. De Nardo,[51a,51b] L. Lista,[51a] D. Monorchio,[51a,51b] G. Onorato,[51a,51b] C. Sciacca,[51a,51b] G. Raven,[52] H. L. Snoek,[52] C. P. Jessop,[53] K. J. Knoepfel,[53] J. M. LoSecco,[53] W. F. Wang,[53] L. A. Corwin,[54] K. Honscheid,[54] H. Kagan,[54] R. Kass,[54] J. P. Morris,[54] A. M. Rahimi,[54] J. J. Regensburger,[54] S. J. Sekula,[54] Q. K. Wong,[54] N. L. Blount,[55] J. Brau,[55] R. Frey,[55] O. Igonkina,[55] J. A. Kolb,[55] M. Lu,[55] R. Rahmat,[55] N. B. Sinev,[55] D. Strom,[55] J. Strube,[55] E. Torrence,[55] G. Castelli,[56a,56b] N. Gagliardi,[56a,56b] M. Margoni,[56a,56b] M. Morandin,[56a] M. Posocco,[56a] M. Rotondo,[56a] F. Simonetto,[56a,56b] R. Stroili,[56a,56b] C. Voci,[56a,56b] P. del Amo Sanchez,[57] E. Ben-Haim,[57] H. Briand,[57] J. Chauveau,[57] O. Hamon,[57] Ph. Leruste,[57] J. Ocariz,[57] A. Perez,[57] J. Prendki,[57] S. Sitt,[57] L. Gladney,[58] M. Biasini,[59a,59b] E. Manoni,[59a,59b] C. Angelini,[60a,60b] G. Batignani,[60a,60b] S. Bettarini,[60a,60b] G. Calderini,[60a,60b,¶] M. Carpinelli,[60a,60b,**] A. Cervelli,[60a,60b] F. Forti,[60a,60b] M. A. Giorgi,[60a,60b] A. Lusiani,[60a,60c] G. Marchiori,[60a,60b] M. Morganti,[60a,60b] N. Neri,[60a,60b] E. Paoloni,[60a,60b] G. Rizzo,[60a,60b] J. J. Walsh,[60a] D. Lopes Pegna,[61] C. Lu,[61] J. Olsen,[61] A. J. S. Smith,[61] A. V. Telnov,[61] F. Anulli,[62a] E. Baracchini,[62a,62b] G. Cavoto,[62a] R. Faccini,[62a,62b] F. Ferrarotto,[62a] F. Ferroni,[62a,62b] M. Gaspero,[62a,62b] P. D. Jackson,[62a] L. Li Gioi,[62a] M. A. Mazzoni,[62a] S. Morganti,[62a] G. Piredda,[62a] F. Renga,[62a,62b] C. Voena,[62a] M. Ebert,[63] T. Hartmann,[63] H. Schröder,[63] R. Waldi,[63] T. Adye,[64] B. Franek,[64] E. O. Olaiya,[64] F. F. Wilson,[64] S. Emery,[65] L. Esteve,[65] G. Hamel de Monchenault,[65] W. Kozanecki,[65] G. Vasseur,[65] Ch. Yèche,[65] M. Zito,[65] X. R. Chen,[66] H. Liu,[66] W. Park,[66] M. V. Purohit,[66] R. M. White,[66]

J. R. Wilson,[66] M. T. Allen,[67] D. Aston,[67] R. Bartoldus,[67] J. F. Benitez,[67] R. Cenci,[67] J. P. Coleman,[67] M. R. Convery,[67] J. C. Dingfelder,[67] J. Dorfan,[67] G. P. Dubois-Felsmann,[67] W. Dunwoodie,[67] R. C. Field,[67] A. M. Gabareen,[67] M. T. Graham,[67] P. Grenier,[67] C. Hast,[67] W. R. Innes,[67] J. Kaminski,[67] M. H. Kelsey,[67] H. Kim,[67] P. Kim,[67] M. L. Kocian,[67] D. W. G. S. Leith,[67] S. Li,[67] B. Lindquist,[67] S. Luitz,[67] V. Luth,[67] H. L. Lynch,[67] D. B. MacFarlane,[67] H. Marsiske,[67] R. Messner,[67] D. R. Muller,[67] H. Neal,[67] S. Nelson,[67] C. P. O'Grady,[67] I. Ofte,[67] M. Perl,[67] B. N. Ratcliff,[67] A. Roodman,[67] A. A. Salnikov,[67] R. H. Schindler,[67] J. Schwiening,[67] A. Snyder,[67] D. Su,[67] M. K. Sullivan,[67] K. Suzuki,[67] S. K. Swain,[67] J. M. Thompson,[67] J. Va'vra,[67] A. P. Wagner,[67] M. Weaver,[67] C. A. West,[67] W. J. Wisniewski,[67] M. Wittgen,[67] D. H. Wright,[67] H. W. Wulsin,[67] A. K. Yarritu,[67] K. Yi,[67] C. C. Young,[67] V. Ziegler,[67] P. R. Burchat,[68] A. J. Edwards,[68] T. S. Miyashita,[68] S. Ahmed,[69] M. S. Alam,[69] J. A. Ernst,[69] B. Pan,[69] M. A. Saeed,[69] S. B. Zain,[69] S. M. Spanier,[70] B. J. Wogsland,[70] R. Eckmann,[71] J. L. Ritchie,[71] A. M. Ruland,[71] C. J. Schilling,[71] R. F. Schwitters,[71] B. W. Drummond,[72] J. M. Izen,[72] X. C. Lou,[72] F. Bianchi,[73a,73b] D. Gamba,[73a,73b] M. Pelliccioni,[73a,73b] M. Bomben,[74a,74b] L. Bosisio,[74a,74b] C. Cartaro,[74a,74b] G. Della Ricca,[74a,74b] L. Lanceri,[74a,74b] L. Vitale,[74a,74b] V. Azzolini,[75] N. Lopez-March,[75] F. Martinez-Vidal,[75] D. A. Milanes,[75] A. Oyanguren,[75] J. Albert,[76] Sw. Banerjee,[76] B. Bhuyan,[76] H. H. F. Choi,[76] K. Hamano,[76] G. J. King,[76] R. Kowalewski,[76] M. J. Lewczuk,[76] I. M. Nugent,[76] J. M. Roney,[76] R. J. Sobie,[76] T. J. Gershon,[77] P. F. Harrison,[77] J. Ilic,[77] T. E. Latham,[77] G. B. Mohanty,[77] E. M. T. Puccio,[77] H. R. Band,[78] X. Chen,[78] S. Dasu,[78] K. T. Flood,[78] Y. Pan,[78] R. Prepost,[78] C. O. Vuosalo,[78] and S. L. Wu[78]

(*BABAR* Collaboration)

[1]*Laboratoire d'Annecy-le-Vieux de Physique des Particules (LAPP), Université de Savoie, CNRS/IN2P3, F-74941 Annecy-Le-Vieux, France*
[2]*Universitat de Barcelona, Facultat de Fisica, Departament ECM, E-08028 Barcelona, Spain*
[3a]*INFN Sezione di Bari, I-70126 Bari, Italy*
[3b]*Dipartmento di Fisica, Università di Bari, I-70126 Bari, Italy*
[4]*University of Bergen, Institute of Physics, N-5007 Bergen, Norway*
[5]*Lawrence Berkeley National Laboratory and University of California, Berkeley, California 94720, USA*
[6]*University of Birmingham, Birmingham, B15 2TT, United Kingdom*
[7]*Ruhr Universität Bochum, Institut für Experimentalphysik 1, D-44780 Bochum, Germany*
[8]*University of British Columbia, Vancouver, British Columbia, Canada V6T 1Z1*
[9]*Brunel University, Uxbridge, Middlesex UB8 3PH, United Kingdom*
[10]*Budker Institute of Nuclear Physics, Novosibirsk 630090, Russia*
[11]*University of California at Irvine, Irvine, California 92697, USA*
[12]*University of California at Los Angeles, Los Angeles, California 90024, USA*
[13]*University of California at Riverside, Riverside, California 92521, USA*
[14]*University of California at San Diego, La Jolla, California 92093, USA*
[15]*University of California at Santa Barbara, Santa Barbara, California 93106, USA*
[16]*University of California at Santa Cruz, Institute for Particle Physics, Santa Cruz, California 95064, USA*
[17]*California Institute of Technology, Pasadena, California 91125, USA*
[18]*University of Cincinnati, Cincinnati, Ohio 45221, USA*
[19]*University of Colorado, Boulder, Colorado 80309, USA*
[20]*Colorado State University, Fort Collins, Colorado 80523, USA*
[21]*Technische Universität Dortmund, Fakultät Physik, D-44221 Dortmund, Germany*
[22]*Technische Universität Dresden, Institut für Kern- und Teilchenphysik, D-01062 Dresden, Germany*
[23]*Laboratoire Leprince-Ringuet, CNRS/IN2P3, Ecole Polytechnique, F-91128 Palaiseau, France*
[24]*University of Edinburgh, Edinburgh EH9 3JZ, United Kingdom*
[25a]*INFN Sezione di Ferrara, I-44100 Ferrara, Italy*
[25b]*Dipartimento di Fisica, Università di Ferrara, I-44100 Ferrara, Italy*
[26]*INFN Laboratori Nazionali di Frascati, I-00044 Frascati, Italy*
[27a]*INFN Sezione di Genova, I-16146 Genova, Italy*
[27b]*Dipartimento di Fisica, Università di Genova, I-16146 Genova, Italy*
[28]*Harvard University, Cambridge, Massachusetts 02138, USA*
[29]*Universität Heidelberg, Physikalisches Institut, Philosophenweg 12, D-69120 Heidelberg, Germany*
[30]*Humboldt-Universität zu Berlin, Institut für Physik, Newtonstraße 15, D-12489 Berlin, Germany*
[31]*Imperial College London, London, SW7 2AZ, United Kingdom*
[32]*University of Iowa, Iowa City, Iowa 52242, USA*
[33]*Iowa State University, Ames, Iowa 50011-3160, USA*
[34]*Johns Hopkins University, Baltimore, Maryland 21218, USA*

[35]Laboratoire de l'Accélérateur Linéaire, IN2P3/CNRS et Université Paris-Sud 11, Centre Scientifique d'Orsay, B.P. 34, F-91898 Orsay Cedex, France
[36]Lawrence Livermore National Laboratory, Livermore, California 94550, USA
[37]University of Liverpool, Liverpool L69 7ZE, United Kingdom
[38]Queen Mary, University of London, London, E1 4NS, United Kingdom
[39]University of London, Royal Holloway and Bedford New College, Egham, Surrey TW20 0EX, United Kingdom
[40]University of Louisville, Louisville, Kentucky 40292, USA
[41]Johannes Gutenberg-Universität Mainz, Institut für Kernphysik, D-55099 Mainz, Germany
[42]University of Manchester, Manchester M13 9PL, United Kingdom
[43]University of Maryland, College Park, Maryland 20742, USA
[44]University of Massachusetts, Amherst, Massachusetts 01003, USA
[45]Massachusetts Institute of Technology, Laboratory for Nuclear Science, Cambridge, Massachusetts 02139, USA
[46]McGill University, Montréal, Québec, Canada H3A 2T8
[47a]INFN Sezione di Milano, I-20133 Milano, Italy
[47b]Dipartimento di Fisica, Università di Milano, I-20133 Milano, Italy
[48]University of Mississippi, University, Mississippi 38677, USA
[49]Université de Montréal, Physique des Particules, Montréal, Québec, Canada H3C 3J7
[50]Mount Holyoke College, South Hadley, Massachusetts 01075, USA
[51a]INFN Sezione di Napoli, I-80126 Napoli, Italy
[51b]Dipartimento di Scienze Fisiche, Università di Napoli Federico II, I-80126 Napoli, Italy
[52]NIKHEF, National Institute for Nuclear Physics and High Energy Physics, NL-1009 DB Amsterdam, The Netherlands
[53]University of Notre Dame, Notre Dame, Indiana 46556, USA
[54]Ohio State University, Columbus, Ohio 43210, USA
[55]University of Oregon, Eugene, Oregon 97403, USA
[56a]INFN Sezione di Padova, I-35131 Padova, Italy
[56b]Dipartimento di Fisica, Università di Padova, I-35131 Padova, Italy
[57]Laboratoire de Physique Nucléaire et de Hautes Energies, IN2P3/CNRS, Université Pierre et Marie Curie-Paris6, Université Denis Diderot-Paris7, F-75252 Paris, France
[58]University of Pennsylvania, Philadelphia, Pennsylvania 19104, USA
[59a]INFN Sezione di Perugia, I-06100 Perugia, Italy
[59b]Dipartimento di Fisica, Università di Perugia, I-06100 Perugia, Italy
[60a]INFN Sezione di Pisa, I-56127 Pisa, Italy
[60b]Dipartimento di Fisica, Università di Pisa, I-56127 Pisa, Italy
[60c]Scuola Normale Superiore di Pisa, I-56127 Pisa, Italy
[61]Princeton University, Princeton, New Jersey 08544, USA
[62a]INFN Sezione di Roma, I-00185 Roma, Italy
[62b]Dipartimento di Fisica, Università di Roma La Sapienza, I-00185 Roma, Italy
[63]Universität Rostock, D-18051 Rostock, Germany
[64]Rutherford Appleton Laboratory, Chilton, Didcot, Oxon, OX11 0QX, United Kingdom
[65]CEA, Irfu, SPP, Centre de Saclay, F-91191 Gif-sur-Yvette, France
[66]University of South Carolina, Columbia, South Carolina 29208, USA
[67]SLAC National Accelerator Laboratory, Stanford, California 94309, USA
[68]Stanford University, Stanford, California 94305-4060, USA
[69]State University of New York, Albany, New York 12222, USA
[70]University of Tennessee, Knoxville, Tennessee 37996, USA
[71]University of Texas at Austin, Austin, Texas 78712, USA
[72]University of Texas at Dallas, Richardson, Texas 75083, USA
[73a]INFN Sezione di Torino, I-10125 Torino, Italy
[73b]Dipartimento di Fisica Sperimentale, Università di Torino, I-10125 Torino, Italy
[74a]INFN Sezione di Trieste, I-34127 Trieste, Italy
[74b]Dipartimento di Fisica, Università di Trieste, I-34127 Trieste, Italy
[75]IFIC, Universitat de Valencia-CSIC, E-46071 Valencia, Spain
[76]University of Victoria, Victoria, British Columbia, Canada V8W 3P6
[77]Department of Physics, University of Warwick, Coventry CV4 7AL, United Kingdom
[78]University of Wisconsin, Madison, Wisconsin 53706, USA

(Received 22 January 2009; published 10 April 2009)

We present improved measurements of the branching fraction $\mathcal{B}$, the longitudinal polarization fraction f_L, and the direct CP asymmetry $\mathcal{A}_{CP}$ in the B meson decay channel $B^+ \to \rho^+\rho^0$. The data sample was collected with the *BABAR* detector at SLAC. The results are $\mathcal{B}(B^+ \to \rho^+\rho^0) = (23.7 \pm 1.4 \pm 1.4) \times 10^{-6}$, $f_L = 0.950 \pm 0.015 \pm 0.006$, and $\mathcal{A}_{CP} = -0.054 \pm 0.055 \pm 0.010$, where the uncertainties are

statistical and systematic, respectively. Based on these results, we perform an isospin analysis and determine the Cabibbo-Kobayashi-Maskawa phase angle $\alpha = \arg(-V_{td}V_{tb}^*/V_{ud}V_{ub}^*)$ to be $(92.4^{+6.0}_{-6.5})^\circ$.

DOI: 10.1103/PhysRevLett.102.141802 PACS numbers: 13.25.Hw, 12.15.Hh, 11.30.Er

In the standard model (SM), the weak interaction couplings of quarks are described by elements V_{ij} of the Cabibbo-Kobayashi-Maskawa (CKM) matrix [1], where $i = u, c, t$ and $j = d, s, b$ are quark indices. The CKM elements are complex, introducing violation of charge-parity (CP) symmetry. Unitarity of the CKM matrix yields a relationship between the V_{ij} that can be represented as a triangle in the complex plane. The SM mechanism for CP violations can be tested through measurement of the sides and angles of this unitarity triangle (UT) [2]. An approximate result $\alpha_{\rm eff}$ for the UT angle $\alpha = \arg(-V_{td}V_{tb}^*/V_{ud}V_{ub}^*)$ can be obtained from B meson decays to CP eigenstates dominated by tree-level $b \to u\bar{u}d$ amplitudes, such as $B \to \rho\rho$ decays (see, e.g., Refs. [2,3]). The correction $\Delta\alpha = \alpha - \alpha_{\rm eff}$, which accounts for loop amplitudes, can be extracted from an analysis of the branching fractions and CP asymmetries of the full set of isospin-related $b \to u\bar{u}d$ channels [4]. One of the most favorable methods to determine α is through an isospin analysis of the $B \to \rho\rho$ system [2,3].

Here we present updated results for the $B^+ \to \rho^+\rho^0$ channel, with $\rho^+ \to \pi^+\pi^0$ and $\rho^0 \to \pi^+\pi^-$, leading to an improved determination of α. Previous studies are presented in Refs. [5,6]. We measure the branching fraction $\mathcal{B}$, the longitudinal polarization fraction f_L, and the direct CP asymmetry $\mathcal{A}_{CP} \equiv (\Gamma_{B^-} - \Gamma_{B^+})/(\Gamma_{B^-} + \Gamma_{B^+})$, with $\Gamma_{B^\pm}$ the $B^\pm$ decay width. Significant deviation of $\mathcal{A}_{CP}$ from the SM prediction of zero could indicate new physics. We also search for the as-yet-unobserved decay $B^+ \to \rho^+ f_0(980)$, with $f_0 \to \pi^+\pi^-$. The use of charge conjugate reactions is implied throughout.

The analysis is based on $(465 \pm 5) \times 10^6$ $B\bar{B}$ events (424 fb^{-1}) collected on the $\Upsilon(4S)$ resonance [center-of-mass (c.m.) energy $\sqrt{s} = 10.58$ GeV] with the *BABAR* detector [7] at the PEP-II asymmetric energy e^+e^- collider at SLAC. Compared to our previous study [5], the analysis incorporates higher signal efficiency and background rejection, twice as much data, and improved procedures to reconstruct charged particles and to account for correlations in the backgrounds. Simulated event samples based on Monte Carlo (MC) event generation are used to determine signal and background characteristics, optimize selection criteria, and evaluate efficiencies.

$B^+ \to \rho^+\rho^0$ decays are described by a superposition of two transversely (helicity ± 1) and one longitudinally (helicity 0) polarized amplitudes. Our acceptance is independent of the angle between the two ρ decay planes in the B rest frame. We integrate over this angle to obtain an expression for $(1/\Gamma)d^2\Gamma/(d\cos\theta_{\rho^0} d\cos\theta_{\rho^+})$:

$$\tfrac{9}{16}[4f_L\cos^2\theta_{\rho^0}\cos^2\theta_{\rho^+} + (1 - f_L)\sin^2\theta_{\rho^0}\sin^2\theta_{\rho^+}], \quad (1)$$

with $f_L \equiv \Gamma_L/\Gamma$, where Γ is the total decay width, Γ_L is the partial width to the longitudinally polarized mode, and the ρ^0 (ρ^+) helicity angle θ_{ρ^0} (θ_{ρ^+}) is the angle between the daughter π^+ in the ρ^0 (ρ^+) rest frame and the direction of the boost from the B^+ rest frame.

A B meson candidate is kinematically characterized by the beam-energy-substituted mass $m_{\rm ES} \equiv \sqrt{s/4 - (p_B^* c)^2}/c^2$ and energy difference $\Delta E \equiv E_B^* - \sqrt{s}/2$, where E_B^* and p_B^* are the c.m. energy and momentum of the B candidate, respectively. Signal events peak at the nominal B mass for $m_{\rm ES}$ and at zero for ΔE, with resolutions of 3 MeV/c^2 and 30 MeV, respectively.

The π^0 mesons are reconstructed through $\pi^0 \to \gamma\gamma$. The γ is required to be consistent with a single electromagnetic shower. The γ and π^0 laboratory energies must be larger than 30 MeV and 0.2 GeV, respectively. The mass of a π^0 candidate (resolution 6 MeV/c^2) is required to lie within $[0.115, 0.150]$ GeV/c^2 and is subsequently constrained to its nominal value [2].

The π^0 (π^-) candidate is combined with a π^+ to form a ρ^+ (ρ^0). The $\pi^\pm$ are identified with measurements of specific energy loss in the tracking chambers and radiation angles and photon multiplicity in a ring-imaging Cherenkov detector [7]. The ρ^+ (ρ^0) candidate mass $m_{\pi^+\pi^0}$ ($m_{\pi^+\pi^-}$) must lie within $[0.52, 1.06]$ GeV/c^2. ρ^+ candidates with misreconstructed π^0 mesons tend to cluster near $\cos\theta_{\rho^+} \approx 1$, so we require $\cos\theta_{\rho^+} \leq 0.8$. The B^+ candidates must satisfy $5.26 < m_{\rm ES} < 5.29$ GeV/c^2 and $|\Delta E| < 0.15$ GeV. In cases of multiple B^+ candidates (about 10% of events), the candidate with the largest B^+ vertex [8] fit probability is retained.

Background from $\bar{B} \to \bar{D}^{(*)}X$ decays, due to $\bar{D}^0 \to K^+\pi^-(\pi^0)$ with kaon misidentification and $\bar{D}^0 \to \pi^+\pi^-\pi^0$, is suppressed by requiring the $K^+\pi^-(\pi^0)$ or $\pi^+\pi^-\pi^0$ invariant mass to lie outside $\pm 4\sigma$ of the nominal D^0 mass [2], with $\sigma \approx 9$ MeV/c^2 the D^0 mass resolution.

The dominant background, from random combinations of particles in continuum events ($e^+e^- \to q\bar{q}$, with $q = u, d, s, c$), is suppressed by requiring $|\cos\theta_T| < 0.8$ [9], with θ_T the angle between the thrust axis of the B candidate's decay products and the thrust axis of the remaining particles in the event (ROE), evaluated in the c.m. frame, and by employing a neural network algorithm based on 11 variables calculated in the c.m.: $|\cos\theta_T|$; the cosines of the angles with respect to the beam axis of the B momentum and B thrust axis (we use the absolute value for the latter variable); the momentum-weighted sums L_0 and L_2 [9], determined with charged and neutral particles separately; the sum of transverse momenta of the ROE particles with respect to the beam axis; the ratio of the second to

zeroth Fox-Wolfram moments [10]; the proper time difference between the B and $\bar{B}$ candidates divided by its uncertainty; and B-tagging information from ROE particles [8]. The neural network output NN peaks near 0 and 1 for continuum and signal events, respectively. We require $NN > 0.2$, which rejects about 5% of the signal and 60% of the continuum events.

We examine the remaining B backgrounds and identify nine channels with peaking structures in $m_{\rm ES}$ or ΔE that can potentially mimic signal events: $B^+ \to \pi^0 a_1^+(1260)$, $\pi^+ a_1^0$, $\rho^0\pi^+\pi^0$, $\rho^+\pi^+\pi^-$, $\rho^-\pi^+\pi^+$, $\pi^0\pi^-\pi^+\pi^+$, $\omega\rho^+$, $f_0\pi^0\pi^+$, and $\eta'\rho^+$, with $a_1 \to \rho\pi$, $\omega \to \pi^+\pi^-$, $f_0 \to \pi^+\pi^-$, and $\eta' \to \gamma\rho^0$. All other B backgrounds are combined into a "nonpeaking" $B\bar{B}$ background component.

An extended unbinned maximum likelihood (ML) fit is applied to the selected events. The fit has 14 components: signal $\rho^+\rho^0$ events, taken to be $B^+ \to \rho^+\rho^0$ events that are correctly reconstructed; self-cross-feed (SxF) events, defined as misreconstructed $B^+ \to \rho^+\rho^0$ events (29% of the $B^+ \to \rho^+\rho^0$ sample); signal $B^+ \to \rho^+ f_0$ events, including both correctly and incorrectly reconstructed events to increase efficiency; nonpeaking $B\bar{B}$ background; continuum background; and the nine peaking $B\bar{B}$ background channels listed above. The $\rho^+\rho^0$ signal and SxF components are further divided into categories with either longitudinal or transverse polarization.

The likelihood function is $\mathcal{L} = (1/N!)\exp(-\sum_j n_j) \times \prod_{i=1}^{N}[\sum_j n_j \mathcal{P}_j(\mathbf{x}_i)]$, with N the number of events, n_j the yield of component j, $\mathcal{P}_j(\mathbf{x}_i)$ the probability density function (PDF) for event i to be associated with component j, and $\mathbf{x}_i$ the seven experimental observables specified in Eq. (2) below. The signal $\rho^+\rho^0$, $\rho^+ f_0$, continuum, and nonpeaking $B\bar{B}$ background yields are allowed to vary in the fit. The $\rho^+\rho^0$ SxF yield is fixed to its expected value based on the MC prediction for the SxF rate and the $B^+ \to \rho^+\rho^0$ branching fraction determined here (we iterate the fit to find this result). The relative contributions of the $\rho^+\rho^0$ longitudinal and transverse polarization components are determined by allowing f_L to vary, with f_L common to the signal and SxF events. The three $\rho\pi\pi$ yields are varied under the requirement that they have the same branching fraction. The $\pi^0 a_1^+$, $\pi^+ a_1^0$, $\omega\rho^+$, and $\eta'\rho^+$ yields are fixed according to their known branching fractions [2]. The $\pi^0\pi^-\pi^+\pi^+$ and $f_0\pi^0\pi^+$ yields are fixed assuming their branching fractions to be 10^{-5}, consistent with or larger than the limits [11,12] for $B^0 \to \pi^+\pi^-\pi^+\pi^+$ and $f_0\pi^+\pi^-$ decays.

About 85% of continuum events, and 90% of nonpeaking $B\bar{B}$ background events, contain at least one misreconstructed ρ. For these events, we find correlations of order 10% between the NN, $m_{\pi\pi}$, and $\cos\theta_\rho$ variables, and—to account for these correlations—construct three-dimensional (3D) PDFs of the five variables based on conditional PDFs $\mathcal{P}(x \mid y)$ of variable x given the value of variable y: $\mathcal{P}_{\rm 3D} = [\mathcal{P}(m_{\pi^+\pi^-} \mid \cos\theta_{\rho^0}) \times \mathcal{P}(\cos\theta_{\rho^0} \mid NN)] \times [\mathcal{P}(m_{\pi^+\pi^0} \mid \cos\theta_{\rho^+}) \times \mathcal{P}(\cos\theta_{\rho^+} \mid NN)] \times \mathcal{P}(NN)$. For example, $\mathcal{P}(m_{\pi^+\pi^0} \mid \cos\theta_{\rho^+})$ is constructed by examining the $m_{\pi^+\pi^0}$ distribution in nine bins of $\cos\theta_{\rho^+}$, fitting a second-order polynomial to each bin, and parameterizing how the coefficients of the polynomial vary between bins. The fraction of events with a correctly reconstructed ρ^+ and ρ^0 is fixed to the MC prediction for the nonpeaking $B\bar{B}$ background and allowed to vary for the continuum background. For all other components, the overall PDFs are defined as the product of seven 1D PDFs, one for each observable. The PDFs of the $\rho^+\rho^0$ signal and SxF helicity angles take the form of Eq. (1), with detector resolution and acceptance incorporated, by summing the longitudinal (L) and transverse (T) components with a relative fraction $f_L\epsilon_L/[f_L\epsilon_L + (1 - f_L)\epsilon_T]$, with ϵ_L and ϵ_T the respective reconstruction efficiencies, leading to an effective 2D PDF in $\cos\theta_{\rho^+}$ and $|\cos\theta_{\rho^0}|$:

$$\mathcal{P}_j(\mathbf{x}_i) = \mathcal{P}_j(m^i_{\rm ES})\mathcal{P}_j(\Delta E^i)\mathcal{P}_j(NN^i)\mathcal{P}_j(m^i_{\pi^+\pi^0}) \times \mathcal{P}_j(m^i_{\pi^+\pi^-})\mathcal{P}_j(\cos\theta^i_{\rho^+}, |\cos\theta^i_{\rho^0}|). \quad (2)$$

The continuum background $m_{\rm ES}$ and ΔE PDFs are derived from a 44 fb^{-1} data sample collected 40 MeV below the $\Upsilon(4S)$ mass. All other PDFs are derived from simulation. For $m_{\rm ES}$, the PDFs of signal and continuum are parameterized by a crystal ball [13] and an ARGUS function [14], respectively. A relativistic Breit-Wigner function with a p-wave Blatt-Weisskopf form factor is used for the $m_{\pi\pi}$ distributions in $\rho^+\rho^0$ signal events. For the background, $m_{\pi\pi}$ is modeled by a combination of a polynomial and the signal function. Slowly varying distributions (ΔE for nonpeaking backgrounds and $\cos\theta_\rho$) are modeled by polynomials. High statistics histograms are used for the NN distributions. The remaining variables are parameterized with sums of Gaussians; e.g., the $m_{\pi\pi}$ distribution in f_0 decays is modeled with a sum of three Gaussians. A large data control sample of $B^+ \to \bar{D}^0\pi^+$ ($\bar{D}^0 \to K^0_S\pi^0$, $K^0_S \to \pi^+\pi^-$) events is used to verify that the resolution and peak position of the signal $m_{\rm ES}$ and ΔE PDFs are accurately simulated.

The fit is applied to the sample of 82 224 selected events. We allow 11 parameters to vary in the fit: five parameters of continuum background PDFs, f_L, and five yields as mentioned above. We find 1122 ± 63(stat) $\rho^+\rho^0$ signal events, 50 ± 30(stat) $\rho^+ f_0$ events, and $f_L = 0.945 \pm 0.015$(stat). The fit provides a simultaneous determination of the number of $B^+ \to \rho^+\rho^0$ and $B^- \to \rho^-\rho^0$ signal events. These fitted yields are used to determine $\mathcal{A}_{CP} = -0.054 \pm 0.055$(stat). Figure 1 shows projections of the $m_{\rm ES}$ and $m_{\pi^+\pi^-}$ distributions. To enhance the visibility of the signal, events are required to satisfy $\mathcal{L}_i(S)/[\mathcal{L}_i(S) + \mathcal{L}_i(B)] > 0.98$, where $\mathcal{L}_i(S)$ is the sum of the likelihood functions for $\rho^+\rho^0$ and $\rho^+ f_0$ signal events excluding the PDF of the plotted variable i and $\mathcal{L}_i(B)$ is the corresponding sum of all other components.

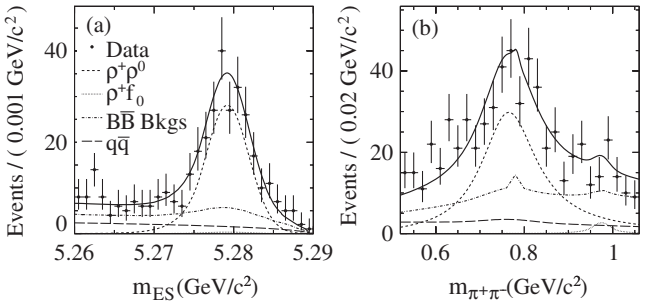

FIG. 1. Projections of the fit (solid curve) onto the (a) $m_{\rm ES}$ and (b) $m_{\pi^+\pi^-}$ variables. A requirement on the likelihood ratio that retains 38% of the signal, 0.1% of the continuum background, and 1.3% of the $B\bar{B}$ background has been applied. The peak in the $B\bar{B}$ background at $m_{\pi^+\pi^-} \approx 0.78$ GeV/c^2 is from $B^+ \to \rho^+\omega$ events with $\omega \to \pi^+\pi^-$.

A possible bias, from unmodeled correlations, is evaluated by applying the ML fit to an ensemble of simulated experiments, where the numbers of signal and background events in each component correspond to those observed or fixed in the fit to data. The continuum events are drawn from the PDFs, while events for all other components are drawn from MC samples. The biases are determined to be 71 ± 3 and -31 ± 1 events for the signal $\rho^+\rho^0$ and ρ^+f_0 yields and -0.005 ± 0.001 for f_L, where the uncertainties are statistical. The signal yields and f_L are then corrected by subtracting these biases.

The branching fractions are given by the bias-corrected yields divided by the reconstruction efficiencies and initial number of $B\bar{B}$ pairs $N_{B\bar{B}}$. From the simulations, the $\rho^+\rho^0$ signal efficiencies including the π^0 daughter branching fraction [2] are $\epsilon_L = [9.12 \pm 0.02(\text{stat})]\%$ and $\epsilon_T = [17.45 \pm 0.03(\text{stat})]\%$. The corresponding result for ρ^+f_0 is $[14.20 \pm 0.08(\text{stat})]\%$. We assume that the $\Upsilon(4S)$ decays to each of B^+B^- and $B^0\bar{B}^0$ 50% of the time.

The principal systematic uncertainties associated with the ML fit are listed in Table I. Uncertainties from the fit biases are defined by the quadratic sum of half the biases themselves (for f_L, the full bias) and the statistical uncertainties of the biases. The uncertainties related to the signal and nonpeaking $B\bar{B}$ background PDFs are assessed by varying the PDF parameters within their uncertainties. For the signal, the uncertainties of the PDF parameters are determined from the $B^+ \to \bar{D}^0\pi^+$ data control sample. Variations of the $\pi^0a_1^+$, $\pi^+a_1^0$, $\omega\rho^+$, and $\eta'\rho^+$ branching fractions within their measured uncertainties, and of the assumed $\pi^+\pi^-\pi^+\pi^0$ and $f_0\pi^+\pi^0$ branching fractions by $\pm 100\%$, define the systematic uncertainty associated with the peaking $B\bar{B}$ background. The uncertainty associated with the SxF fraction is assessed by varying the fixed SxF yield by $\pm 10\%$. The other principal sources of systematic uncertainty are the π^0 reconstruction efficiency (3.0%), the track reconstruction efficiency (1.1%), the $\pi^\pm$ identification efficiency (1.5%), the uncertainty of $N_{B\bar{B}}$ (1.1%), and the selection requirements on $|\cos\theta_T|$ (1.0%). The individual terms are added in quadrature to define the total systematic uncertainties.

TABLE I. Principal systematic uncertainties associated with the ML fit (in events for the $\rho^+\rho^0$ and ρ^+f_0 yields).

	$\rho^+\rho^0$ yield	ρ^+f_0 yield	f_L	$\mathcal{A}_{CP}$
Fit biases	35.5	15.3	0.005	0.001
Signal PDFs	19.4	3.0	0.001	0.002
Nonpeaking $B\bar{B}$ PDFs	7.3	2.1	0.001	0.001
Peaking $B\bar{B}$ yields	16.3	21.1	0.003	0.001
SxF fraction	7.9	0.1	0.001	0.001

We find $\mathcal{B}(B^+ \to \rho^+\rho^0) = (23.7 \pm 1.4 \pm 1.4) \times 10^{-6}$, $f_L = 0.950 \pm 0.015 \pm 0.006$, $\mathcal{A}_{CP} = -0.054 \pm 0.055 \pm 0.010$, and $\mathcal{B}(B^+ \to \rho^+f_0) \times \mathcal{B}(f_0 \to \pi^+\pi^-) = (1.21 \pm 0.44 \pm 0.40) \times 10^{-6}$, where the first (second) uncertainty is statistical (systematic). The $\mathcal{B}(\rho^+\rho^0)$ result is larger than in Ref. [5], primarily because of the improved method used here to account for correlations in the backgrounds. The significance of the $\mathcal{B}(\rho^+f_0)$ result without (with) systematics is 3.2 (2.2) standard deviations. We find $-0.15 < \mathcal{A}_{CP} < 0.04$ and $\mathcal{B}(B^+ \to \rho^+f_0) \times \mathcal{B}(f_0 \to \pi^+\pi^-) < 2.0 \times 10^{-6}$, where these latter results correspond to the 90% confidence level (C.L.) including systematics.

We perform an isospin analysis of $B \to \rho\rho$ decays by minimizing a χ^2 that includes the measured quantities expressed as the lengths of the sides of the B and $\bar{B}$ isospin triangles [4]. We use the $B^+ \to \rho^+\rho^0$ branching fraction and f_L results presented here, with the branching fractions, polarizations, and CP-violating parameters in $B^0 \to \rho^+\rho^-$ [15] and $B^0 \to \rho^0\rho^0$ [11] decays. We assume the uncertainties to be Gaussian-distributed and neglect potential isospin $I = 1$ and electroweak-loop amplitudes, which are expected to be small [3].

The CKM phase angle α and its correction $\Delta\alpha$ are found to be $\alpha = (92.4^{+6.0}_{-6.5})^\circ$ and $-1.8^\circ < \Delta\alpha < 6.7^\circ$, respectively, at 68% C.L., significant improvements [16] compared to $\alpha = (82.6^{+32.6}_{-6.3})^\circ$ and $|\Delta\alpha| < 15.7^\circ$ [11] obtained with the same $\rho^+\rho^-$ and $\rho^0\rho^0$ measurements, but the previous $B^+ \to \rho^+\rho^0$ results [5], or $\alpha = (91.7 \pm 14.9)^\circ$ from the Belle Collaboration [12]. The improvement is primarily due to the increase in $\mathcal{B}(\rho^+\rho^0)$ compared to our previous result. $\mathcal{B}(\rho^+\rho^0)$ determines the length of the common base of the isospin triangles for the B and $\bar{B}$ decays. The increase in the base length flattens both triangles, making the four possible solutions [4] nearly degenerate.

In summary, we have improved the precision of the measurements of the $B^+ \to \rho^+\rho^0$ decay branching and longitudinal polarization fractions, leading to a significant improvement in the determination of the CKM phase angle α based on the favored $B \to \rho\rho$ isospin method. We set a

90% C.L. upper limit of 2.0×10^{-6} on the branching fraction of $B^+ \to \rho^+ f_0(980)$, with $f_0 \to \pi^+\pi^-$.

We are grateful for the excellent luminosity and machine conditions provided by our PEP-II colleagues and for the substantial dedicated effort from the computing organizations that support *BABAR*. The collaborating institutions thank SLAC for its support and kind hospitality. This work is supported by DOE and NSF (USA), NSERC (Canada), CEA and CNRS-IN2P3 (France), BMBF and DFG (Germany), INFN (Italy), FOM (The Netherlands), NFR (Norway), MES (Russia), MEC (Spain), and STFC (United Kingdom). Individuals have received support from the Marie Curie EIF (European Union) and the A. P. Sloan Foundation.

*Present address: Temple University, Philadelphia, PA 19122, USA.

†Present address: Tel Aviv University, Tel Aviv, 69978, Israel.

‡Also at Università di Perugia, Dipartimento di Fisica, Perugia, Italy.

§Also at Università di Roma La Sapienza, I-00185 Roma, Italy.

‖Present address: University of South Alabama, Mobile, AL 36688, USA.

¶Also at Laboratoire de Physique Nucléaire et de Hautes Energies, IN2P3/CNRS, Université Pierre et Marie Curie-Paris6, Université Denis Diderot-Paris7, F-75252 Paris, France.

**Also at Università di Sassari, Sassari, Italy.

[1] N. Cabibbo, Phys. Rev. Lett. **10**, 531 (1963); M. Kobayashi and T. Maskawa, Prog. Theor. Phys. **49**, 652 (1973).

[2] C. Amsler *et al.* (Particle Data Group), Phys. Lett. B **667**, 1 (2008).

[3] J. Charles *et al.* (CKMFitter Group), Eur. Phys. J. C **41**, 1 (2005); M. Bona *et al.* (UTfit Collaboration), J. High Energy Phys. 03 (2006) 080.

[4] M. Gronau and D. London, Phys. Rev. Lett. **65**, 3381 (1990); H. Lipkin *et al.*, Phys. Rev. D **44**, 1454 (1991).

[5] B. Aubert *et al.* (*BABAR* Collaboration), Phys. Rev. Lett. **97**, 261801 (2006).

[6] B. Aubert *et al.* (*BABAR* Collaboration), Phys. Rev. Lett. **91**, 171802 (2003); J. Zhang *et al.* (Belle Collaboration), Phys. Rev. Lett. **91**, 221801 (2003).

[7] B. Aubert *et al.* (*BABAR* Collaboration), Nucl. Instrum. Methods Phys. Res., Sect. A **479**, 1 (2002).

[8] B. Aubert *et al.* (*BABAR* Collaboration), Phys. Rev. Lett. **94**, 161803 (2005).

[9] B. Aubert *et al.* (*BABAR* Collaboration), Phys. Rev. D **70**, 032006 (2004).

[10] G. C. Fox and S. Wolfram, Nucl. Phys. **B149**, 413 (1979).

[11] B. Aubert *et al.* (*BABAR* Collaboration), Phys. Rev. D **78**, 071104 (2008).

[12] C.-C. Chiang *et al.* (Belle Collaboration), Phys. Rev. D **78**, 111102 (2008).

[13] M. J. Oreglia, Ph.D. thesis [SLAC Report No. SLAC-R-236, 1980], Appendix D; J. E. Gaiser, Ph.D. thesis [SLAC Report No. SLAC-R-255, 1982], Appendix F; T. Skwarnicki, Ph.D. thesis [DESY Report No. F31-86-02, 1986], Appendix E.

[14] H. Albrecht *et al.* (ARGUS Collaboration), Phys. Lett. B **241**, 278 (1990).

[15] B. Aubert *et al.* (*BABAR* Collaboration), Phys. Rev. D **76**, 052007 (2007).

[16] See EPAPS Document No. E-PRLTAO-102-007918 for confidence level plots illustrating the improvements in α and $\Delta\alpha$ due to this analysis. For more information on EPAPS, see http://www.aip.org/pubservs/epaps.html.